Research Square

Preprints are preliminary reports that have not undergone peer review.
They should not be considered conclusive, used to inform clinical practice,
or referenced by the media as validated information.

Safety Profile of Stem Cell-Derived Secretome: Ocular and Systemic Evaluation in Rats

Alícia Sousa Moreira
LAQV, REQUIMTE, Instituto de Ciências Biomédicas de Abel Salazar, Universidade do Porto

Bruna Lopes
LAQV, REQUIMTE, Instituto de Ciências Biomédicas de Abel Salazar, Universidade do Porto

Ana Catarina Sousa
LAQV, REQUIMTE, Instituto de Ciências Biomédicas de Abel Salazar, Universidade do Porto

Patrícia Sousa
LAQV, REQUIMTE, Instituto de Ciências Biomédicas de Abel Salazar, Universidade do Porto

Beatriz Rosa Silva
Associate Laboratory for Animal and Veterinary Sciences (AL4AnimalS), Faculdade de Medicina Veterinária (FMV), Universidade de Lisboa (UL), Avenida da Universidade Técnica, 1300-477 Lisboa, Portugal

Gonçalo Santos
Associate Laboratory for Animal and Veterinary Sciences (AL4AnimalS), Faculdade de Medicina Veterinária (FMV), Universidade de Lisboa (UL), Avenida da Universidade Técnica, 1300-477 Lisboa, Portugal

Rodrigo Marques
Associate Laboratory for Animal and Veterinary Sciences (AL4AnimalS), Faculdade de Medicina Veterinária (FMV), Universidade de Lisboa (UL), Avenida da Universidade Técnica, 1300-477 Lisboa, Portugal

Irina Amorim
Departamento de Patologia e Imunologia Molecular, Instituto de Ciências Biomédicas de Abel Salazar (ICBAS), Universidade do Porto (UP), Porto, Portugal

João R. Mesquita
LAQV, REQUIMTE, Instituto de Ciências Biomédicas de Abel Salazar, Universidade do Porto

Esmeralda Delgado
Centro de Investigação Interdisciplinar em Sanidade Animal

Rui Alvites
Cooperativa de Ensino Superior Politécnico e Universitário (CESPU), Gandra PRD, Portugal

Ana Colette Maurício
acmauricio@icbas.up.pt

LAQV, REQUIMTE, Instituto de Ciências Biomédicas de Abel Salazar, Universidade do Porto

Research Article

Keywords: secretome/conditioned medium, glaucoma, ocular tolerance, electroretinography, mesenchymal stromal cells, subconjunctival/intravitreal route

Posted Date: July 31st, 2026

DOI: https://doi.org/10.21203/rs.3.rs-10108290/v1

License: This work is licensed under a Creative Commons Attribution 4.0 International License. Read Full License

Additional Declarations: No competing interests reported.

Safety Profile of Stem Cell-Derived Secretome: Ocular and Systemic Evaluation in Rats

Alícia de Sousa Moreira[1,2], Bruna Lopes[1,2], Ana Catarina Sousa[1,2,3,4], Patrícia Sousa[1,2], Beatriz Rosa Silva[5,6,7], Gonçalo Santos[5,6,7], Rodrigo Marques[5,7], Irina Amorim[9,10], João R. Mesquita[1,2], Esmeralda Delgado[5,6,7], Rui Alvites[1,2,11] and Ana Colette Maurício[1,2*]

[1]LAQV, REQUIMTE, Instituto de Ciências Biomédicas de Abel Salazar, Universidade do Porto, Rua de Jorge Viterbo Ferreira, 228, 4050-313 Porto, Portugal; alicia.moreira.1998@gmail.com (A.D.S.M.); brunisabel95@gmail.com (B.L.); anacatarinasoaressousa@hotmail.com (A.C.S.); pfrfs_10@hotmail.com (P.S.); jrmesquita@icbas.up.pt (J.R.M.); ruialvites@hotmail.com (R.A.); acmauricio@icbas.up.pt (A.C.M.);
[2]Departamento de Clínicas Veterinárias, Instituto de Ciências Biomédicas de Abel Salazar (ICBAS), Universidade do Porto (UP), Porto, Portugal;
[3]RISE-Health, School of Medicine and Biomedical Sciences, Fernando Pessoa University, Fernando Pessoa Teaching and Culture Foundation, Gondomar, Portugal;
[4]Biomedical and Health Sciences (FP-BHS), Instituto de Investigação, Inovação e Desenvolvimento Fernando Pessoa (FP-I3ID), Fundação Ensino e Cultura Fernando Pessoa, Porto, Portugal;
[5]Centro de Investigação Interdisciplinar em Sanidade Animal (CIISA), Faculdade de Medicina Veterinária (FMV), Universidade de Lisboa (UL), Portugal; brsilva.fmv@gmail.com (B.R.S.);
[6]Hospital Escolar Veterinário (HEV), Faculdade de Medicina Veterinária (FMV), Universidade de Lisboa (UL), Portugal;
[7]Associate Laboratory for Animal and Veterinary Sciences (AL4AnimalS), Faculdade de Medicina Veterinária (FMV), Universidade de Lisboa (UL), Avenida da Universidade Técnica, 1300-477 Lisboa, Portugal; goncalospinolavet@hotmail.com (G.S.); rmarques2001@gmail.com (R.M.); esmeralda@fmv.ulisboa.pt (E.D.);
[8]Research Institute for Medicines (iMed.ULisboa), Faculdade de Farmácia (FFUL), Universidade de Lisboa (UL), Lisboa, Portugal;
[9]Instituto de Investigação e Inovação (i3S), Universidade do Porto (UP), Porto, Portugal, ifamorim@icbas.up.pt (I.A.);
[10]Departamento de Patologia e Imunologia Molecular, Instituto de Ciências Biomédicas de Abel Salazar (ICBAS), Universidade do Porto (UP), Porto, Portugal;
[11]Cooperativa de Ensino Superior Politécnico e Universitário (CESPU), Gandra PRD, Portugal.

* **Correspondence**: acmauricio@icbas.up.pt.

Tel.: +351-919071286 or +351-220428000

Abstract

Stem cell-based therapies have gained recently increasing attention as potential treatment options for retinal diseases, including glaucoma. Among these approaches, the secretome or the conditioned medium (CM) derived from mesenchymal stromal cells (MSCs) represents a promising cell-free therapeutic alternative due to its regenerative and immunomodulatory properties. However, prior to exploring therapeutic efficacy in animal disease models, its ocular and systemic safety must be established. The present study aimed to evaluate the tolerance of human umbilical cord (hUC) MSCs-derived CM following subconjunctival (SbC) and intravitreal (ITV) administration in healthy Wistar Hannover rats. Twenty-four adult male rats were

randomly assigned to four experimental groups based on administration route (SbC or ITV) and euthanasia timepoint (5 or 28 days). CM was administered unilaterally to the right eye, with the contralateral eye serving as an internal control. Ocular tolerance was assessed through comprehensive ophthalmic examination, intraocular pressure (IOP) monitoring, electroretinography (ERG), and histological evaluation of ocular tissues. Systemic safety was evaluated through histopathological analysis of liver, kidney, and spleen samples. No relevant persistent ocular abnormalities or sustained IOP changes were observed. Retinal function remained largely preserved, although ITV administration induced mild alterations in selected electrophysiological parameters. Histological analysis revealed overall preservation of the retinal architecture, despite a reduction in outer nuclear layer thickness in ITV groups at the later timepoint. Histopathological examination of systemic organs showed preserved tissue architecture with only mild incidental findings. Overall, these results support the ocular and systemic tolerability of MSCs CM in healthy rats, with SbC delivery showing a more stable functional and structural profile.

Keywords: secretome/conditioned medium, glaucoma, ocular tolerance, electroretinography, mesenchymal stromal cells, subconjunctival/intravitreal route.

1. Introduction

Retinal diseases encompass a heterogeneous group of degenerative and ischemic conditions that lead to retinal cell apoptosis and progressive loss of retinal structural integrity. Among these diseases, diabetic retinopathy, age-related macular degeneration, retinitis pigmentosa and glaucoma, are particularly relevant, as they represent major causes of irreversible visual impairment and blindness worldwide, with glaucoma being especially significant in both human and canine patients (1–5).

Glaucoma is a leading cause of irreversible blindness and chronic pain worldwide. This disease is characterized by progressive optic neuropathy, in which apoptosis of retinal ganglion cells (RGCs) results in gradual vision loss. Once initiated, RGCs degeneration continues and is accompanied by progressive structural and functional alterations in the optic nerve head, including optic disc cupping and thinning of both the retinal nerve fiber layer and the neuroretinal rim, reflecting the chronic and progressive nature of this disease (6).

Current therapeutic strategies for glaucoma primarily focus on lowering intraocular pressure (IOP) through pharmacological, laser, or surgical approaches. Although these interventions can delay the disease progression, they do not directly target neurodegeneration or promote retinal neuroprotection and tissue repair. Consequently, vision loss may continue despite adequate IOP control, highlighting the need for alternative therapeutic strategies targeting neuroprotection and neuroregeneration (7,8).

Lately, regenerative medicine and cell-based therapies have emerged as promising tools in ophthalmic research, especially regarding retinal diseases, with increasing interest in stem cells or their bioproducts. Several therapeutic strategies have been explored, including stem cell transplantation as well as cell-free approaches based on stem cell-derived products, such as secretome and extracellular vesicles, including exosomes (9,10). These approaches aim to exploit the regenerative and immunomodulatory properties of stem cells while avoiding some of the limitations associated with direct cell transplantation, such as ethical concerns, tumorigenic potential, or immune rejection. Growing evidence indicates that the secretome released by mesenchymal stromal cells (MSCs) contains a complex mixture of bioactive factors, cytokines, growth factors, and chemokines, capable of modulating inflammation (11),

supporting neuronal survival by inhibiting apoptosis (12) and fibrosis (13), while maintaining retinal homeostasis. Consequently, MSC-derived secretome has emerged as a promising complementary therapeutic strategy in glaucoma research.

Accordingly, the aim of this study was to evaluate the ocular and systemic tolerance of human umbilical cord (hUC)-MSCs secretome following subconjunctival (SbC) or intravitreal (ITV) administration in healthy Wistar Hannover adult male albino rats. Conditioned medium (CM) refers to the culture medium enriched with factors released by cells, under controlled in vitro conditioning settings (in vitro preconditioning), whereas the term secretome more precisely describes the full spectrum of bioactive molecules actively secreted by those cells (14–17). These factors are produced in response to specific environmental stimuli or stressors, such as hypoxia, priming with cytokines, or nutrient deprivation, which can enhance their immunomodulatory, neuroprotective, and tissue repair properties (16,17). Establishing the safety and tolerability of these cell-free products under physiological conditions is a critical step before exploring their therapeutic potential in experimental disease models, including glaucoma.

2. Materials and Methods

2.1 Animals and Ethical Approval

All experimental procedures involving animals were reviewed and approved by the Organism Responsible for Animal Welfare (ORBEA) of the Faculdade de Medicina Veterinária, University of Lisbon (FMV-ULisboa) (Project No./Ref. 005/2023/ORBEA-FMV-ULisboa), as well as by the General Directorate of Food and Veterinary (Direção Geral de Alimentação e Veterinária – DGAV). All experiments were conducted in compliance with national legislation (Decree-Law No. 113/2013) and with Directive 2010/63/EU of the European Parliament, and followed the OECD Guidance Document

on the Recognition, Assessment and Use of Clinical Signs as Humane Endpoints for Experimental Animals in Safety Evaluation (2000), and the ARRIVE 2.0 guidelines. Every effort was made to minimize animal discomfort and pain, and predefined humane endpoints were strictly applied to safeguard animal welfare. In accordance with the principles of Replacement, Reduction and Refinement (3Rs), the same cohort of animals was used to obtain data for two complementary experimental studies, thereby reducing the total number of animals required while maximizing the scientific output from each subject.

2.2 Reagents, drugs and equipment

Healthy adult male Wistar Hannover rats (mean body weight of 330 ± 55 g), obtained from Charles River Laboratories (Barcelona, Spain), were included in this study. Before the inclusion, all animals underwent a complete ophthalmic examination, and those without ocular abnormalities were selected. All ophthalmic examinations and experimental procedures were performed at the Faculty of Veterinary Medicine, University of Lisbon, using dedicated equipment, including a rebound tonometer (Tonolab®, Icare, Finland), an electroretinography system (RETIcom, Roland Consult, Stasche & Finger GmbH, Brandenburg, Germany), a slit lamp (Hawk Eye®, Dioptrix, France), a PanOptic® ophthalmoscope (WelchAllynHillrom, Chicago, IL, USA), a binocular magnifier (Carl Zeiss®, Oberkochen, Germany) and a surgical microscope (OPMI Lumera i®, Carl Zeiss Surgical GmbH, Germany).

CM was obtained from hUC-MSCs acquired from a certified commercial supplier (PromoCell®, Heidelberg, Germany), which had been previously fully characterized *in vitro* (18,19). Cells were expanded under standard culture conditions, and CM was collected and stored after 48 hours according to previously established and validated protocols of the research group (19,20).

All pharmacological drugs used in this study were available at the FMV-ULisboa. These included ketamine (Ketamidor® 100 mg/mL, Richter Pharma, Wels, Austria), medetomidine (Domitor® 1 mg/mL, Orion Corporation, Espoo, Finland), atipamezole (Antisedan® 5 mg/mL, Zoetis, NJ, USA), sodium pentobarbital (Euthasol® 400 mg/mL, Animalcare Group, North Yorkshire, UK), oxybuprocaine hydrochloride (Anestocil®, Edol, Lisbon, Portugal), and a carbomer-based ocular gel (Lubrithal®, Dechra, Northwich, UK). Histological processing of tissue sections, including hematoxylin and eosin (H&E) staining, was performed using a Thermo Scientific Gemini™ AS slide stainer (MA, USA).

2.3 Experimental Design

A total of 24 male Wistar Hannover adult rats were randomly allocated into four experimental groups (n = 6 per group) using a simple randomization procedure prior to CM administration. The number of animals included in each group was defined based on previous ocular tolerance studies and ethical considerations in accordance with the principles of Reduction (3Rs), aiming to minimize animal use while ensuring adequate assessment of ocular and systemic safety endpoints. Animals were housed in type IV cages (floor area: 1875 cm^2) fitted with stainless-steel wire lids. Animals had ad libitum access to standard laboratory chow and water, adapted to their physiological needs. Housing conditions were controlled, with a 12 h light/dark cycle, ambient temperature maintained at 20 ± 2 °C, and relative humidity ranging between 50 and 60%.

Experimental groups were defined according to the route of CM administration and the euthanasia timepoint. CM was administered unilaterally to the right eye (OD) of each animal, either through the SbC route (Groups 1 and 2) or the ITV route (Groups 3 and 4). Animals were euthanized at 5 days (Groups 1 and 3) or 28 days (Groups 2 and

4) post-administration. The contralateral (left) eye (OS) did not receive CM and served as an internal control for each animal.

The primary outcome measures were retinal function (Electroretinography – ERG), IOP and retinal histological integrity. Secondary outcome measures included clinical ophthalmic findings and histopathological evaluation of systemic organs.

2.4 Ophthalmic examination

Prior to study inclusion, all animals (n = 24) underwent a complete ophthalmic evaluation. This assessment included intraocular pressure (IOP) measurement using a rebound tonometer (Tonolab®, Icare, Finland), slit-lamp biomicroscopic examination of the anterior segment (Hawk Eye®, Dioptrix, France), and fundoscopic evaluation of the posterior segment using a PanOptic® ophthalmoscope (Welch Allyn–Hillrom, Skaneateles Falls, NY, USA). No animals or data points were excluded after group allocation, and all animals completed the study protocol.

Following CM administration, complete ophthalmic examinations were carried out at predefined timepoints, namely at 5 and 28 days post-administration. In animals receiving ITV injections, IOP was measured immediately after CM administration and again 1h post-procedure to monitor for potential transient changes associated with the invasiveness of this route. Additionally, in all animals, IOP measurements were performed at 1 and 2 days following CM administration.

2.5 Electroretinography (ERG)

ERG is a widely used method to assess retinal function by measuring its electrical response to light stimuli. In this study, ERG was employed to evaluate the impact of different CM administration routes on retinal function in healthy rats, to determine which administration route would be the safest approach (SbC or ITV).

Flash ERG recordings were obtained in all animals at two time points: baseline recording (prior to CM administration) to confirm normal retinal function, and the

second recording was performed prior to euthanasia. The ERG protocol followed established methodologies previously described in the literature (21,22), allowing for the evaluation of rod and cone activity through measurements of a-wave and b-wave amplitudes (in μV) in response to light stimuli. Animals were dark-adapted for 12 hours (overnight) before each ERG session.

General anesthesia was required to guarantee total immobilization during the procedure, using an intraperitoneal injection of ketamine (70 mg/kg) and medetomidine (0.8 mg/kg). Active electrodes with silver wire tips were positioned on the corneas of both eyes (**Figure 1-A**) after the application of one drop of oxybuprocaine (Anestocil®, Edol, Lisbon, Portugal), followed by a drop of a lubricant carbomer-based gel (Lubrithal®, Dechra, Northwich, United Kingdom) to ensure proper contact and corneal lubrication.

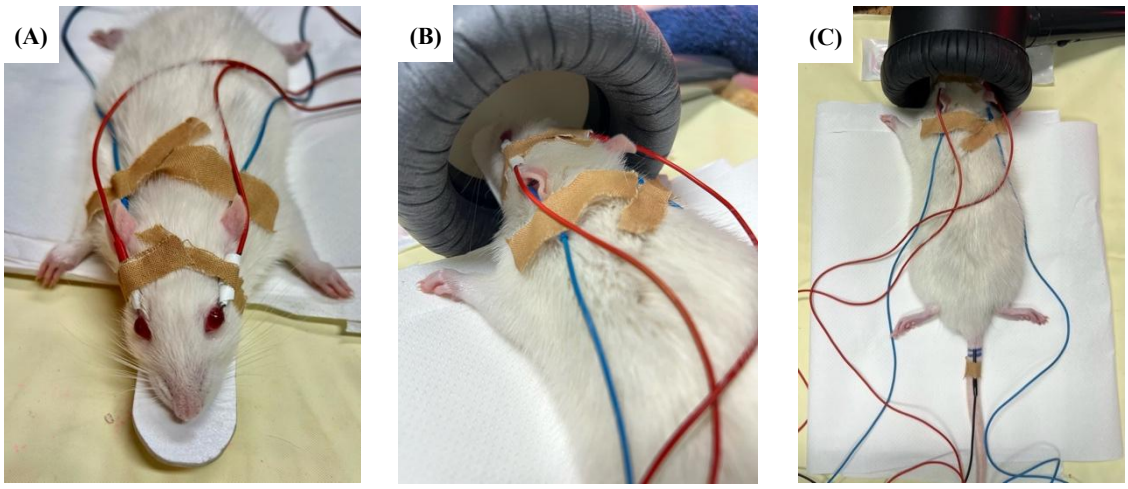


Figure 1. Electroretinography (ERG) set: (A) active electrodes (red) with silver tips placed on corneas; (B) reference electrodes (blue) placed next to the ears and head positioning inside the MiniGanzfeld stimulator; (C) ground electrode (black) placed at the base of the tail and the final ERG electrode and stimulator positioning.

Reference electrodes were inserted subcutaneously, with their tips placed between the ear and lateral canthus on both sides of the head, while the ground electrode was positioned at the base of the tail (**Figure 1-C**). A heating pad was used to maintain the animal's body temperature, which was regularly monitored. For light stimulation, a

Mini Ganzfeld device was fitted over the animal's head (**Figure 1-B and 1-C**). Signals were recorded separately for each eye, ensuring impedance values below 5 kΩ within a frequency range of 0.1–1000 Hz (with 0 dB corresponding to 3 cd·s/m²).

Each ERG session lasted approximately 75 minutes and was divided into five phases. The first phase, scotopic luminance response (SLR), included nine flash intensities ranging from –35 dB to +5 dB, each delivered three times at a frequency of 0.1 Hz. This was followed by the photopic adaptation (PA) phase, where the flash intensity was based on the maximum b-wave amplitude obtained in the SLR. Flashes were applied three times at 1.3 Hz at 0, 2, 4, 8, and 16 minutes of light adaptation.

The third phase, photopic luminance response (PLR), involved light flashes of nine different intensities (from –35 dB to +5 dB), delivered three times at 1.3 Hz after light adaptation. Then, the photopic flicker phase presented flashes at 0, –5, –10, and –15 dB, delivered at 6.3 Hz following 10 minutes of light exposure. The final phase, scotopic adaptation (SA), used dim white flashes delivered three times at 1.3 Hz at 0, 2, 4, 8, 16, and 32 minutes of dark adaptation.

Rod function was evaluated using low-intensity flashes under dark-adapted conditions -scotopic - (–35 dB = –3.02 log cd·s/m²), while cone function was assessed through exposure to high-intensity flashes (+5 dB = 0.98 log cd·s/m²) and 6.3 Hz flicker stimulation under light-adapted (photopic) conditions.

In summary, the ERG protocol comprised the following phases:

1. SLR: Assessing rod photoreceptor response at increasing light intensities;
2. PA: Measuring cone function at different adaptation times;
3. PLR: Evaluating cone photoreceptor response at increasing light intensities;
4. PF: Assessing response to flickering light stimuli;
5. SA: Measuring rod function over time.

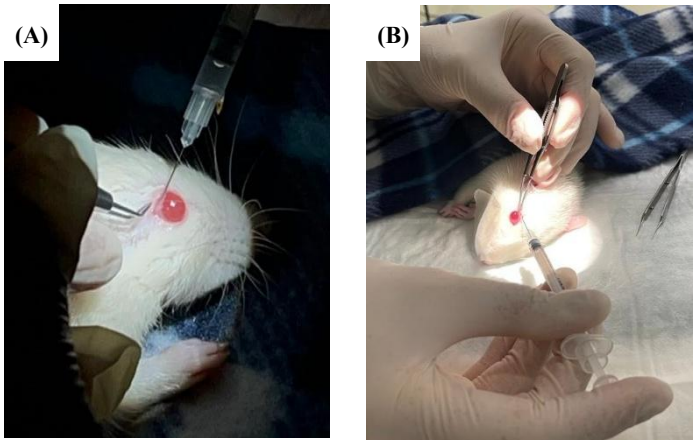
For each ERG phase, data were recorded separately for the OD and OS, analyzing both a-wave (photoreceptor response) and b-wave (bipolar cell response).

2.6 CM production and administration

hUC-MSCs were expanded under standard culture conditions until reaching 70-80% confluence. Cells were then washed with a phosphate buffered saline solution (PBS), and CM was generated by incubating the cells in serum-free DMEM/F12 GlutaMAX™ medium (10565018, Gibco®) for 48 h. After collection, CM was centrifuged to remove cellular debris, and the resulting supernatant was stored frozen at −80 °C until further use.

At the end of the baseline ERG, after confirming normal retinal function, SbC or ITV administration of hUC-MSC–derived CM was performed under anesthesia, according to group allocation. CM was administered unilaterally to the OD, while the OS served as an untreated negative control. Due to the nature of the procedures, investigators performing CM administration and ophthalmic examinations were aware of group allocation.

SbC administration (**Figure 2-A**) was carried out using an insulin syringe fitted with a 29-gauge needle, with a total volume of 50 µL delivered across three distinct SbC sites under binocular magnification. ITV injections (**Figure 2-B**) were performed under a



surgical microscope, with a total injection volume of 5 μL. At the end of the procedure, anesthesia was reversed by subcutaneous administration of atipamezole (2.5 mg/kg).

Figure 2. SbC (A) and ITV (B) administration of CM from hUC-MSCs in the OD of two rats, under general anesthesia.

2.7 Euthanasia and Tissue Collection

Animals were euthanized at predefined timepoints: 5 days (n = 12) and 28 days (n = 12) following CM administration. Euthanasia was performed by intraperitoneal administration of sodium pentobarbital (150 mg/kg). Prior to euthanasia, animals underwent a second ERG evaluation under anesthesia. Immediately after euthanasia, both eyes were carefully enucleated. The optic nerve and globe orientation were marked using tissue dyes to ensure correct anatomical orientation during histological processing (**Figure 3**). Enucleated eyes were fixed by intraocular injection and immersion in 10% (v/v) formaldehyde and subsequently embedded in paraffin.

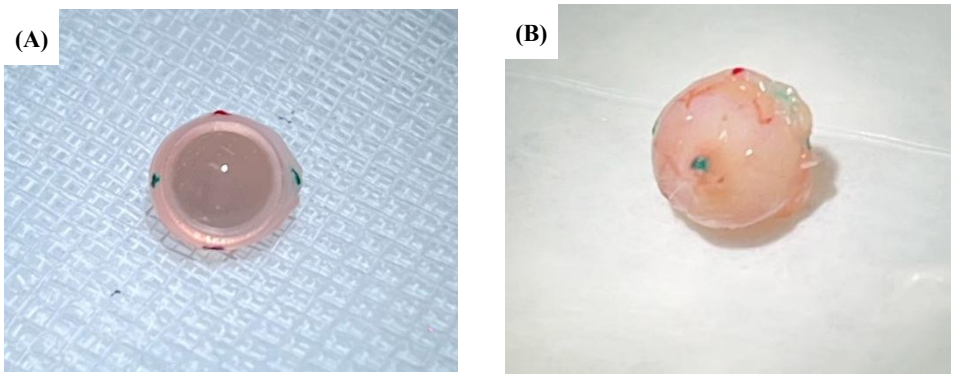


Figure 3. Orientation of the rat ocular globe using tissue dyes. Tissue dyes were applied immediately after enucleation to preserve anatomical orientation during histological processing. Red dye was placed on the dorsal surface of the globe, blue dye on the ventral surface, and green dye on the medial and lateral aspects, shown in the frontal view (A). In the caudal view (B), the green-marked area allows identification of the transected optic nerve, facilitating consistent orientation of histological sections.

In addition, liver, kidney, and spleen samples were collected at the time of euthanasia to assess potential systemic toxicity or histopathological alterations associated with CM administration.

2.8 Histological Evaluation

Following paraffin embedding of the ocular globes, routine histological processing was performed using hematoxylin and eosin (H&E) staining. Serial transverse sections of 3 μm thickness were obtained from both eyes using a microtome, and four

representative sections per eye were selected for comprehensive histopathological assessment. The resulting H&E-stained slides were subsequently digitized using a whole-slide imaging system. Histological measurements were performed in a blinded manner using coded digital slides.

Digital retinal thickness measurements were performed using QuPath (version 0.6.0, University of Edinburgh, UK). Histological evaluation focused on three predefined parameters: total retinal thickness, inner nuclear layer (INL) thickness, and outer nuclear layer (ONL) thickness. All measurements were conducted in a standardized and blinded manner, with comparisons made between treated and contralateral control eyes, between administration routes (SbC vs. ITV), and between euthanasia timepoints (5 vs. 28 days).

In addition, the representative samples from the liver, kidneys, and spleen were formalin-fixed, paraffin-embedded, sectioned, and stained with H&E to assess potential systemic toxicity or treatment-related histopathological alterations associated with CM administration.

2.9 Statistical Analysis

Data were analyzed using GraphPad Prism 10 (version 10.5.0; GraphPad Software, La Jolla, CA, USA). Retinal thickness measurements were obtained using QuPath (version 0.6.0; University of Edinburgh, UK) and subsequently analyzed in GraphPad Prism.

IOP measurements obtained at baseline (day 0), day 1, day 2, and at euthanasia, were analyzed using two-way ANOVA to assess the effects of time and experimental group, followed by Tukey's multiple comparisons test.

ERG data were analyzed using simple linear regression to model the relationship between stimulus intensity/time and ERG wave amplitude. Comparisons between experimental groups were performed by evaluating differences in regression slopes and fitted curves, where applicable.

Retinal layers thicknesses were analyzed using two-way ANOVA to evaluate the effects of administration route (SbC vs. ITV), time point (5 vs. 28 days), and eye (OD vs. control OS). Multiple comparisons were performed using Tukey's multiple comparisons test for overall group comparisons and Šídák's multiple comparisons test for predefined pairwise comparisons, including treated versus control eyes, administration routes, and timepoints.

Differences were considered statistically significant at $p < 0.05$. Statistical significance is indicated in the figures using one, two, three, or four asterisks corresponding to $0.01 \leq p < 0.05$; $0.001 \leq p < 0.01$; $0.0001 \leq p < 0.001$; and $p < 0.0001$, respectively.

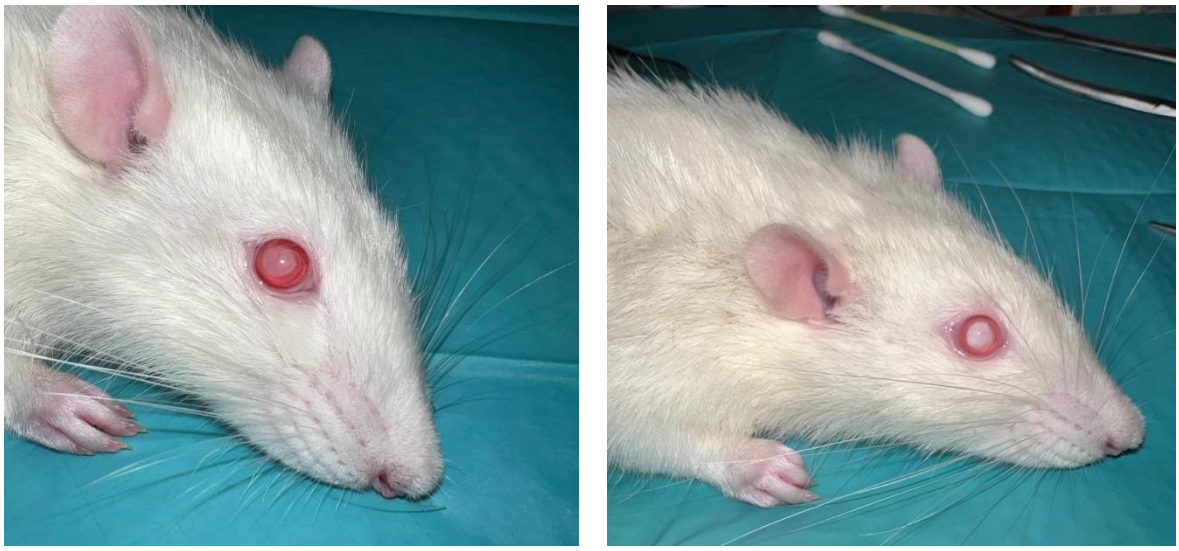
Morphological evaluation of ocular tissues and systemic organs (spleen, liver, and kidney) was performed descriptively based on histological examination.

316 Statistical analyses were conducted using anonymized datasets whenever
317 possible.

318 ## 3. Results

319 *3.1 Ophthalmic examination*

320 Preliminary tolerance evaluations showed no significant alterations in animal well-
321 being following CM administration, using the Grimace scale. No ocular surface or
322 anterior chamber abnormalities were observed throughout the study, except for two
323 cases of cataracts. Those animals developed unilateral mature cataracts during the
324 follow-up period, clinically characterized as complete lens opacification and
325 subsequent leucocoria in the right eye following ITV CM administration (**Figure 4**).



326 **Figure 4. Right unilateral leucocoria due to a total mature cataract that developed in two rats after**
327 **ITV administration of CM.**

328 Slit-lamp examination revealed no conjunctival hyperemia, chemosis, corneal edema,
329 epithelial defects, anterior chamber flare, hyphema, or hypopyon.

330 Fundoscopic evaluation showed no retinal detachment, vitreous opacities,
331 hemorrhages, vascular abnormalities, or optic nerve head alterations in any of the
332 examined eyes.

All animals maintained normal behavior and showed no signs of ocular pain or distress during the experimental period.

3.2 IOP measurements

Before CM administration, the mean IOP was 12.08 ± 2.11 mmHg in the OD and 12.88 ± 2.37 mmHg in the OS, measured immediately after sedation. At the time of euthanasia, mean IOP values were 10.96 ± 1.29 mmHg (OD) and 11.50 ± 0.69 mmHg (OS). Occasional values fell below 10 mmHg, which was considered expected under sedation and consistent with the experimental conditions.

Baseline IOP values were comparable between OD and OS and remained within the physiological range (10-20 mmHg) throughout the study. As illustrated in **Figure 5**, IOP values in treated eyes exhibited mild fluctuations over time across all groups. Although some variability was observed between timepoints, no progressive IOP increase was detected following CM administration via either SbC (Groups 1 and 2) or ITV (Groups 3 and 4) routes. Group 2 presented higher mean IOP values at baseline and at day 2 compared to the remaining groups. However, these values decreased by the time of euthanasia. Group 3 showed a transient reduction on day 1 followed by gradual stabilization overtime, while Groups 1 and 4 demonstrated relatively stable IOP values.

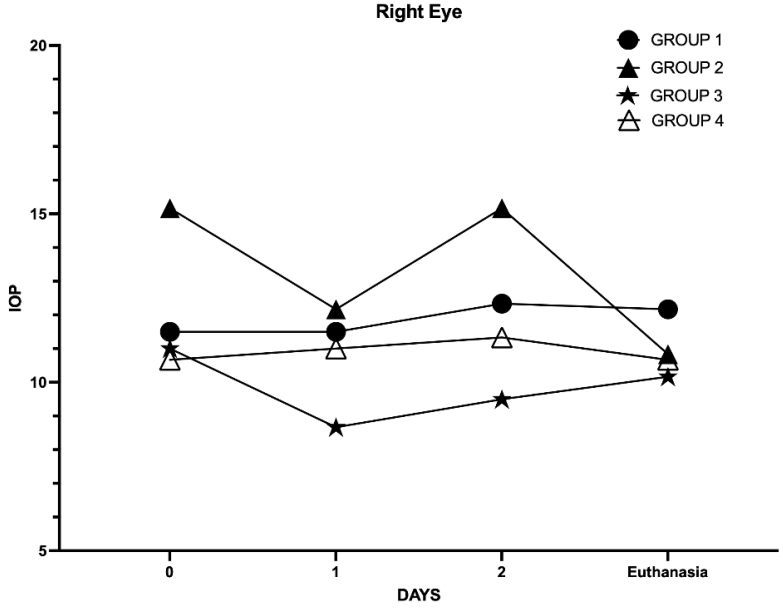


Figure 5. Evolution of IOP in the OD across experimental groups. The graph illustrates the mean IOP values (mmHg) for the treated eye in all groups at different timepoints: Day 0 (before CM administration), Day 1, Day 2, and euthanasia. Each line represents a specific experimental group, where OD received the CM via SbC (Groups 1 and 2) or ITV (Groups 3 and 4) route. The data highlight trends and variations in IOP over time, with all groups maintaining values largely within or near the physiological range for Wistar Hannover rats (10-20 mmHg). Significant variations are noted within certain groups but remain consistent with the experimental setup and sedation conditions.

Statistical comparisons within OD values are shown in **Figure 6**. Significant differences between specific time points were identified within certain groups. These differences were observed primarily between baseline and later time points and between day 2 and euthanasia. However, these variations were transient and not indicative sustained IOP elevation. Importantly, all values remained within the expected physiological range for sedated animals.

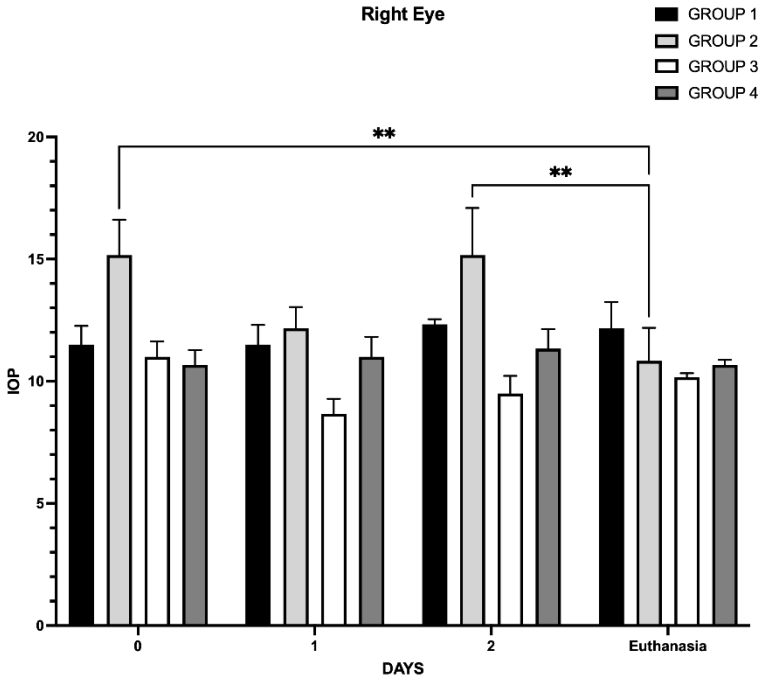


Figure 6. Intra-group statistical comparisons of IOP in the OD across experimental groups. Bar graph representing the mean IOP values (mmHg) for the OD in all experimental groups at different timepoints: Day 0 (before CM administration), Day 1, Day 2, and euthanasia. Groups 1 and 2 received CM via the SbC route, whereas Groups 3 and 4 received CM via the ITV route. Bars represent mean ± SD. Statistically significant differences between specific timepoints within the same group are indicated by ** ($0.001 \leq p < 0.01$), as determined by two-way ANOVA followed by appropriate post hoc comparisons. Despite statistically significant variations, IOP values remained within the physiological range for Wistar Hannover rats under sedation.

In the OS, temporal patterns were similar, as depicted in **Figure 7**. Mild fluctuations were observed, particularly in Groups 1 and 2, which showed slightly higher baseline values followed by a reduction at euthanasia. Groups 3 and 4 remained comparatively stable throughout the study.

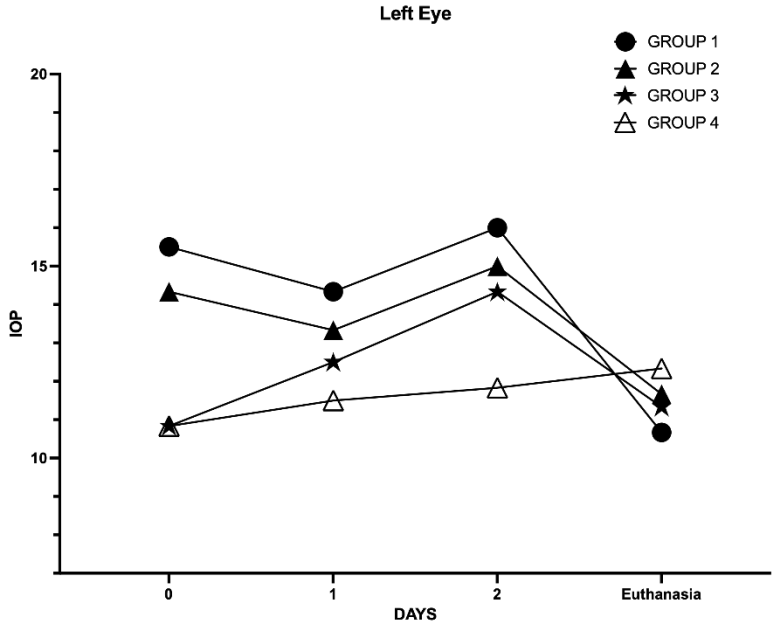


Figure 7. Evolution of IOP in the OS across experimental groups. Line graph illustrating the mean IOP values (mmHg) for the OS in all experimental groups at different timepoints: Day 0, Day 1, Day 2, and euthanasia. The OS served as an internal control and did not receive CM administration. Groups 1 and 2 correspond to the SbC route, while Groups 3 and 4 correspond to the ITV route in the OD. The data demonstrate mild temporal fluctuations, with values remaining largely within the physiological range for Wistar Hannover rats (10–20 mmHg), consistent with the experimental and sedation conditions.

As shown in **Figure 8**, statistically significant differences between selected time points were also detected within certain control groups. Nevertheless, these changes were not progressive and did not indicate persistent deviation from physiological IOP levels. Given that OS did not receive CM administration, these variations are most likely attributable to physiological variability and sedation rather than treatment-related alterations.

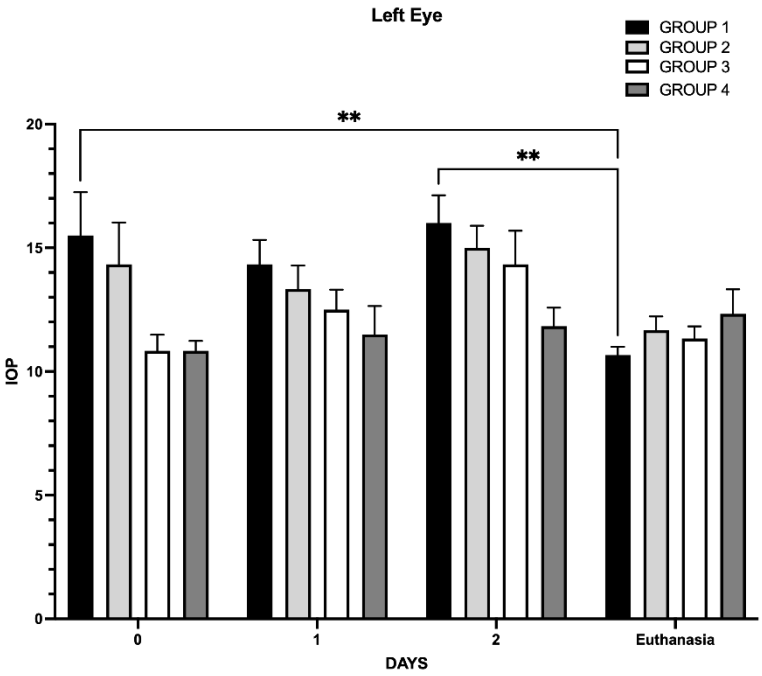


Figure 8. Intra-group statistical comparisons of IOP in the OS across experimental groups. Bar graph representing the mean IOP values (mmHg) for the OS across all experimental groups at the evaluated timepoints. The values are represented as mean ± SD. Statistically significant differences between selected timepoints within the same group are indicated by ** ($0.001 \leq p < 0.01$), as determined by two-way ANOVA followed by appropriate post hoc testing. As the OS did not receive CM administration, the observed variations likely reflect physiological variability and the effects of sedation rather than treatment-related alterations. All values remained within the expected physiological range.

3.3 Electroretinography (ERG)

To further explore functional retinal tolerance following CM administration, the relationship between stimulus intensity (or adaptation time) and ERG amplitude was analyzed using linear regression models. This approach enabled a detailed assessment of how the retinal response pattern evolved before and after treatment, providing complementary information to the amplitude and IOP results previously described.

Linear regression analysis were performed for each experimental group, ERG phase and wave (a- and b-waves). Slopes of the intensity-response (or time-response, in adaptation stages) correlations obtained before and after CM administration were

compared within each group, to determine whether CM administration induced retinal functional alterations.

Although most slope comparisons did not have statistical significance, visual inspection of regression plots revealed subtle curve displacements and amplitude variations between pre- and post-treatment recordings, particularly in the ITV groups. These tendencies, while not statistically confirmed, may reflect minor fluctuations in retinal excitability or adaptive responses following CM exposure. Overall, the absence of measurable slope differences supports preserved retinal function for most conditions. All slope values are summarized in **Table 1**, and detailed regression plots comparisons are provided in **Supplementary Material (Figures S1 – non-significant comparison – and S2 to S12 – significant comparisons – detailed in 3.3.1 and 3.3.2).**

To address the two main objectives of this study, only the statistically significant comparisons between pre- and post-treatment regressions, are described below, including: (1) the comparison between SbC and ITV administration at each timepoint (5 and 28 days), and (2) the comparison between timepoints (5 vs. 28 days) within each route.

3.3.1 Comparison of administration routes

Retinal responses obtained after SbC and ITV CM administration were compared.

3.3.1.1 Subconjunctival vs. Intravitreal administration at 5 days:

3.3.1.1.1 SLR wave a – SbC vs ITV

Linear regression analysis of the a-wave amplitude in the SLR stage was performed to compare retinal function before and five days after CM administration for each delivery route (**Figure S2 – Supplementary Material**).

In the SbC group, slopes did not differ significantly (p = 0.1554), indicating that the relation between light intensity and photoreceptor response remained stable after treatment. The high coefficients of determination (R^2 = 0.82 before and R^2 = 0.78 after)

confirmed a strong and consistent correlation between stimulus intensity and retinal response, reinforcing photoreceptors stability.

In contrast, the ITV group showed a highly statistically significant difference between slopes ($p < 0.0001$), revealing a marked alteration in the intensity-response correlation, despite presenting high determination coefficients ($R^2 = 0.80$ before and $R^2 = 0.82$ after).

3.3.1.1.2 PLR wave b – SbC vs ITV

Linear regression analysis of the b-wave amplitude in the photopic luminescent response (PLR) phase was performed to compare retinal function before and five days after CM administration for each route of delivery (**Figure S3 – Supplementary Material**).

In the SbC group, the regression lines were nearly superimposed ($p = 0.8429$), indicating no significant changes in the intensity-response relationship, suggesting stable retinal behaviour after treatment. Consistently, the coefficients of determination revealed a low correlation before ($R^2 = 0.21$) and a moderate one after the administration ($R^2 = 0.58$). This reinforces the interpretation of preserved and even slightly improved response predictability in the SbC group.

Conversely, the intravitreally treated group exhibited a significant difference between slopes ($p = 0.0265$), reflecting an altered response pattern, with R^2 markedly decreased from 0.57 before to 0.23 after treatment, denoting an increased variability of the retinal response.

3.3.1.1.3 PF wave b – SbC vs ITV

Linear regression analysis of the b-wave amplitude in the PF phase was performed to compare retinal function before and five days after CM administration for each route of delivery (**Figure S4 – Supplementary Material**).

In the SbC group, the slope of the intensity–response curve remained unaffected after treatment ($p = 0.3400$), which indicates a stable flicker response and preserved retinal

function. The coefficients of determination were both moderate before ($R^2 = 0.52$) and after treatment ($R^2 = 0.43$), revealing consistency between stimulus intensity and response amplitude, although slightly less robust after CM administration. This may suggest a mildly variable pattern in retinal response.

In contrast, the ITV treated group exhibited a significant difference between slopes ($p = 0.0251$), revealing an altered intensity-response relation after CM injection. In this group, the R^2 decreased from 0.62 before to 0.35 after treatment, indicating a weakening of the stimulus intensity-retinal response correlation.

3.3.1.2 Subconjunctival vs. Intravitreal administration at 28 days

3.3.1.2.1 SLR wave b – SbC vs ITV

Linear regression analysis of the b-wave amplitude in the SLR phase was performed to evaluate long-term retinal function before and twenty-eight days after CM administration (**Figure S5 – Supplementary Material**).

In the SbC group, no significant difference was detected between pre- and post-treatment slopes ($p = 0.3462$), suggesting a sustained functional integrity of rod-driven pathways following SbC delivery. The determination coefficients decreased from $R^2 = 0.47$ before to $R^2 = 0.23$ after treatment, indicating a weaker correlation between light intensity and response amplitude, therefore a slightly higher variability among individual responses. Nevertheless, the absence of slope changes support preserved global retinal behavior.

Conversely, the ITV group exhibited a significant difference between slopes ($p = 0.0074$), demonstrating an altered intensity-response profile after CM administration, and also a markedly decreased of R^2 from 0.63 to 0.28.

3.3.1.2.2 SLR wave a – SbC vs ITV

Linear regression analysis of the a-wave amplitude in the SLR step was performed to assess potential long-term alterations in outer retinal function after CM administration (**Figure S6 – Supplementary Material**).

SbC group showed no significant slope differences (p = 0.0753), indicating that the photoreceptor-driven response remained stable over the 28-day period. The determination coefficients were high before (R^2 = 0.76) and after treatment (R^2 = 0.79), confirming a strong correlation between light intensity and response amplitude, and suggesting a sustained and reliable photoreceptor performance over time.

In contrast, the ITV group exhibited a major significant difference between slopes (p < 0.0001), demonstrating a marked alteration in the intensity-response effect following CM administration. Despite the high R^2 values (0.82 before and 0.73 after) a slight reduction was observed, and together with the significantly flatter slope, indicates that the intensity-response relationship remained strong but shifted in magnitude, reflecting a real functional alteration rather than random variability.

3.3.1.2.3 SA wave a – SbC vs ITV

Linear regression analysis of the a-wave amplitude in the SA stage was performed to evaluate long-term retinal responses to sustained dark adaptation following CM administration (**Figure S7 – Supplementary Material**).

In the SbC group, a significant difference between pre- and post-treatment slopes (p = 0.0129), indicated and altered relationship between adaptation time and photoreceptor response after CM delivery. However, low and identical R^2 values (0.28), suggest that this change reflects a weak correlation and likely represents a subtle, variable trend rather than a strong or consistent effect.

The steeper post-treatment slope may reflect a mild increase in retinal excitability or an adaptive improvement in photoreceptor sensitivity following SbC injection.

On the other hand, the ITV group showed no significant slope differences ($p = 0.6890$), indicating stable dark-adaptation behaviour and consistent photoreceptor responses across timepoints. Very low R^2 values (0.12 before and 0.17 after) further confirm the absence of a meaningful correlation, consistent with stable and non-responsive retinal behaviour under scotopic conditions.

3.3.2 Comparison of timepoints

To evaluate whether retinal responses changed over time after CM administration, slope comparisons were performed between the 5-day and 28-day timepoints within each administration route.

3.3.2.1 Subconjunctival administration — 5 days vs. 28 days

3.3.2.1.1 SA wave a – SbC 5 days vs. SbC 28 days

In the SA stage, a-wave slopes differed significantly between 5 and 28 days ($p = 0.0129$), with a steeper slope at day 28, indicating a more pronounced increase in a-wave amplitude during dark adaptation (**Figure S8 – Supplementary Material**).

However, the coefficients of determination remained low at both timepoints ($R^2 = 0.11$ and 0.08 at 5 days; $R^2 = 0.28$ before and after at 28 days), indicating weak correlations and high variability. Therefore, this change likely reflects a mild adaptive trend rather than a consistent or strong functional improvement.

3.3.2.2 Intravitreal administration — 5 days vs. 28 days

3.3.2.2.1 SLR wave b – ITV 5 days vs. ITV 28 days

In the SLR stage, the b-wave slopes showed no difference at 5 days ($p = 0.1466$) but differed significantly at 28 days ($p = 0.0074$), indicating a time-dependent alteration in the scotopic response (**Figure S9 – Supplementary Material**).

3.3.2.2.2 SLR wave a – ITV 5 days vs. ITV 28 days

The a-wave slopes in the SLR stage, showed significant differences both at 5 days ($p < 0.0001$) and at 28 days ($p < 0.0001$) after ITV CM administration (**Figure S10 – Supplementary Material**).

The 28-day regression displayed a flatter slope and lower overall amplitudes, suggesting progressive reduction in photoreceptor responsiveness. The coefficients of determination were high at all timepoints ($R^2 = 0.80$ and 0.82 at 5 days; $R^2 = 0.82$ and 0.73 at 28 days), indicating strong and consistent correlations between light intensity and a-wave amplitude. This confirms that the observed differences in slope are not due to random variability but reflect genuine functional alterations in the outer retina.

3.3.2.2.3 PLR wave b – ITV 5 days vs. ITV 28 days

In the PLR stage, a significant slope difference was observed at 5 days ($p = 0.0265$) on wave b, but not at 28 days ($p = 0.0993$) following ITV CM administration (**Figure S11 – Supplementary Material**).

This pattern suggests an initial alteration in the photopic intensity-response relationship, which tended to normalize over time. Consistently, R^2 values showed a marked decline at 5 days (0.57 before vs. 0.23 after), indicating a transient disruption and increased variability in the light intensity-b-wave amplitude relationship shortly after injection. By contrast, at 28 days, R^2 values improved (0.29 before and 0.40 after), showing a modest recovery of correlation strength and reduced response dispersion. This R^2 pattern supports the idea of an early, short-lived functional disturbance followed by gradual reestablishment of cone-driven retinal stability.

By 28 days, the b-wave responses appeared more stable, indicating a partial functional recovery of the cone-driven retinal pathways.

3.3.2.2.4 PF wave b – ITV 5 days vs. ITV 28 days

In the PF stage, a significant slope difference was detected at 5 days ($p = 0.0251$), but not at 28 days ($p = 0.9292$) on wave b after ITV CM administration (**Figure S12 – Supplementary Material**).

At the 5-day timepoint, there is a clear reduction in correlation strength ($R^2 = 0.62$ before vs. 0.35 after), indicating increased variability and transient disturbance of the flicker response immediately after injection. By contrast, at 28 days, R^2 values improved from 0.22 before to 0.50 after treatment, revealing a partial recovery of the relationship between stimulus intensity and response amplitude. Altogether, these findings indicate a transient functional disturbance following ITV administration, with early post-injection effects that resolved over time, consistent with overall retinal tolerance.

3.4 Histological Evaluation

3.4.1 Retinal Thickness Measurements

Histological evaluation of H&E-stained ocular sections demonstrated overall preservation of retinal architecture across all experimental groups. No evidence of cellular degeneration, tissue disorganization, inflammatory cell infiltration, or other morphological abnormalities was detected. Retinal lamination remained intact, with well-defined nuclear layers and preserved structural integrity. Additionally, no qualitative

differences were observed between OD and OS eyes within any group. Representative H&E-stained microscopic images of the ocular tissues are presented in Figure 9.

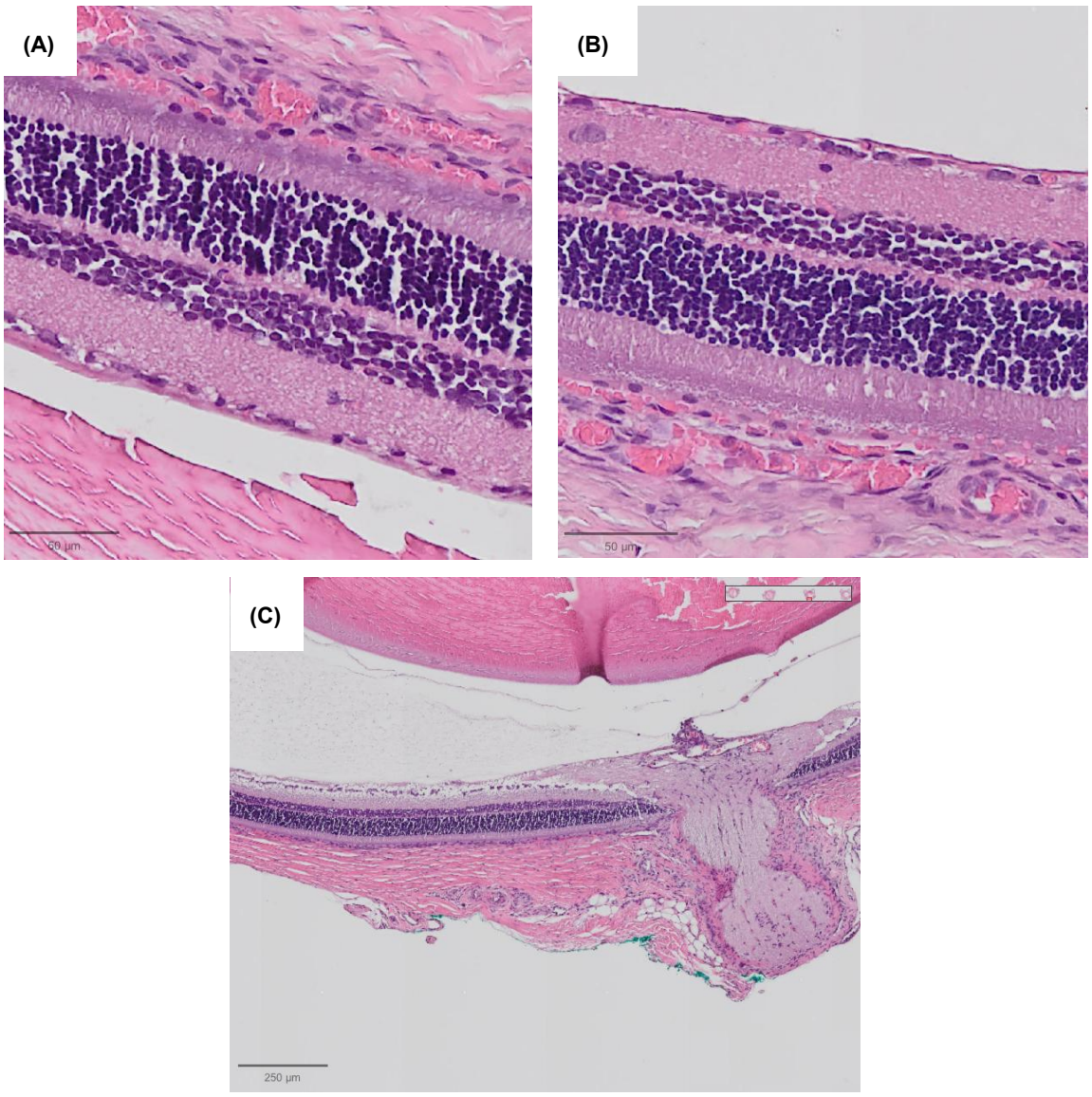


Figure 9. Representative photomicrographs of retinal sections demonstrating preserved retinal architecture. (A) OS and (B) OD sections showing well-maintained retinal lamination, with clearly defined nuclear layers and no evidence of tissue disorganization or inflammatory infiltration. (C) Section including the optic nerve head region, illustrating the transition between the neurosensory retina and the optic nerve. The green tissue dye visible in this area corresponds to the orientation marker applied during sample processing, as previously described in Figure 3. Whole-slide images were digitally scanned and visualized using QuPath software, with representative regions of interest subsequently selected and captured. H&E staining; 20× magnification.

3.4.1.1 Comparison between eyes (OD vs. OS)

No statistically significant differences were detected between OD and OS in any experimental group for any of the retinal thickness parameters assessed (INL, ONL, or total retinal thickness) ($p > 0.05$ for all comparisons) (**Figure 10**).

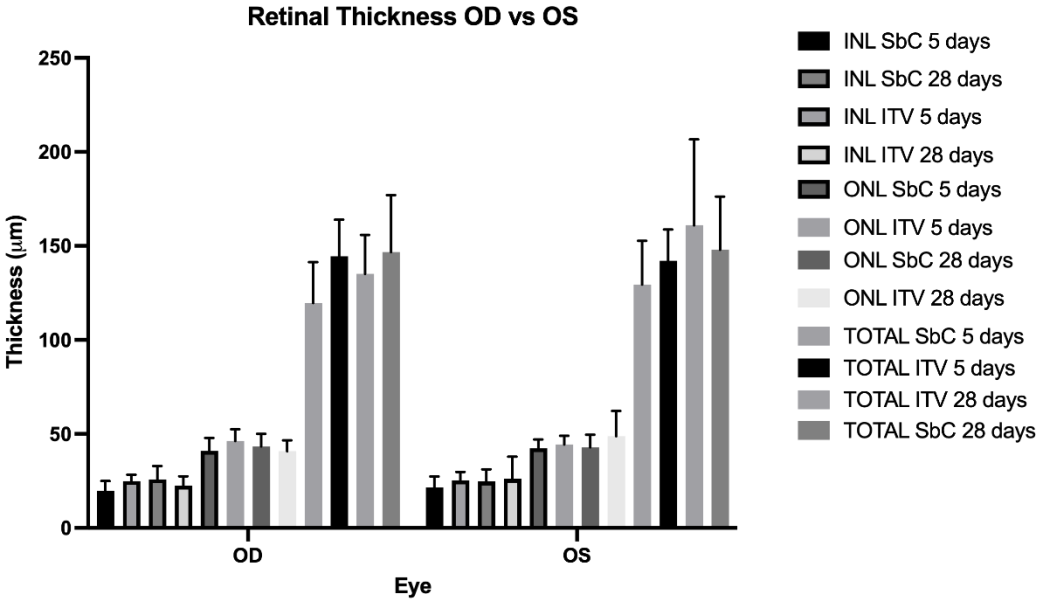


Figure 10. Retinal thickness comparison between OD and OS. Histological evaluation of retinal thickness included three parameters: inner nuclear layer (INL), outer nuclear layer (ONL), and total retinal thickness (TOTAL). Comparisons were performed between OD and OS, considering the administration routes SbC and ITV, and euthanasia timepoints at 5 and 28 days. Data are presented as mean ± SEM. No statistically significant differences were detected between OD and OS within any experimental group for INL, ONL, or TOTAL thickness ($p > 0.05$ in all cases).

3.4.1.2 Comparison between administration routes (SbC vs. ITV) and euthanasia timepoints (5 vs. 28 days)

INL thickness remained largely consistent across experimental groups (**Figure 11**). A modest but statistically significant reduction was detected in the ITV group at 28 days

when compared with the SbC group at the same timepoint ($p = 0.0356$). All other pairwise comparisons involving the INL thickness were not statistically significant ($p > 0.05$).

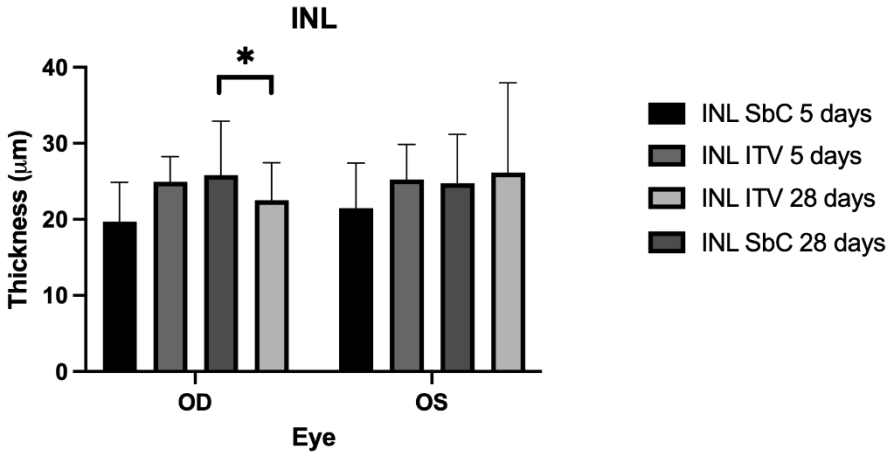


Figure 11. INL thickness across administration routes and timepoints. Quantitative histological measurements of INL thickness (μm) were obtained from OD and OS following subconjunctival (SbC) or intravitreal (ITV) administration of the secretome at 5 and 28 days post-administration. Data are presented as mean ± SEM. INL thickness remained largely stable across experimental conditions. A modest but statistically significant reduction was detected in the ITV 28-day group compared with the SbC 28-day group ($p = 0.0356$; indicated by *). All other pairwise comparisons, including those between the 5- and 28-day timepoints within each administration route, were not statistically significant ($p > 0.05$).

ONL thickness was significantly reduced in the ITV groups, with the most pronounced decrease at the 28-day timepoint (**Figure 12**). The comparison between ITV 28 days and SbC 28 days revealed a highly significant difference ($p < 0.0001$), with similar findings in other comparisons involving the ITV 28-day group. In contrast, no statistically significant differences were detected between the subconjunctival groups at 5 and 28 days ($p > 0.05$).

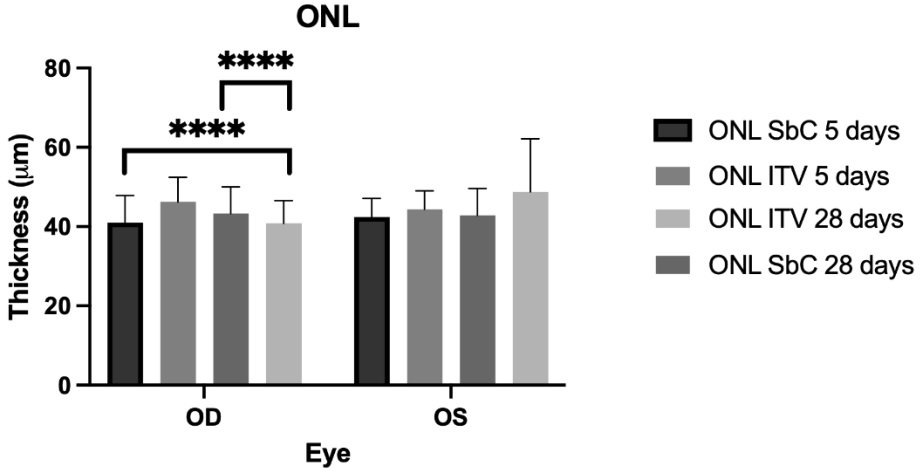


Figure 12. ONL thickness across administration routes and timepoints. Histological quantification of ONL thickness (μm) was performed in OD and OS following SbC or ITV administration at 5 and 28 days post-injection. Data are presented as mean ± SEM. ONL thickness was significantly reduced in the ITV groups, particularly at 28 days. Comparison between ITV 28 days and SbC 28 days revealed a highly significant reduction (****, $p < 0.0001$). Similar significant differences were observed in other comparisons involving the ITV 28-day group. No statistically significant differences were detected between SbC groups at 5 and 28 days ($p > 0.05$).

Total retinal thickness exhibited a pattern similar to that observed for the ONL (**Figure 13**). The ITV groups, particularly at the 28-day timepoint, showed a marked reduction in retinal thickness compared with the SbC groups at both timepoints ($p < 0.0001$). No significant differences were detected between 5 and 28 days within the SbC groups ($p > 0.05$), whereas a significant decrease over time was observed within the ITV group ($p < 0.01$).

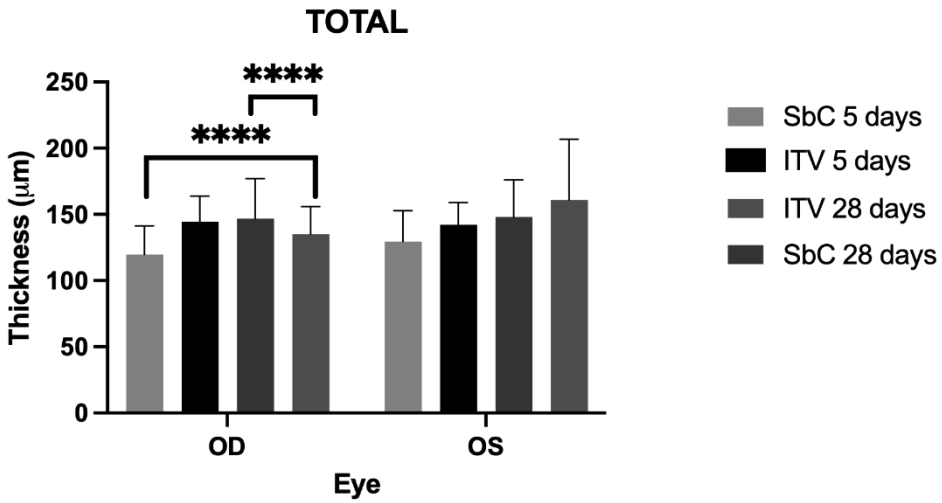


Figure 13. Total retinal thickness across administration routes and timepoints. Histological quantification of total retinal thickness (μm) was performed in OD and OS following SbC or ITV administration at 5- and 28-days post-injection. Data are presented as mean ± SEM. Total retinal thickness followed the same pattern observed for ONL. The ITV groups, particularly at 28 days, exhibited a significant reduction in thickness compared with the SbC groups at both 5 and 28 days (****, $p < 0.0001$). Within each administration route, no statistically significant differences were detected between the 5- and 28-day timepoints for SbC delivery ($p > 0.05$), whereas a significant decrease from 5 to 28 days was observed in the ITV group ($p < 0.01$).

3.4.2 Histopathological evaluation of systemic organs

Overall, liver, kidney, and spleen architecture was preserved, with no evidence of severe lesions or systemic toxicity. However, mild histopathological alterations were identified.

In the kidney, the cortical and medullary regions maintained normal structural organization. Mild, multifocal chronic interstitial nephritis was occasionally observed, characterized by sparse interstitial inflammatory infiltrates. Rare hyaline casts were present within renal tubules, and mild generalized vascular congestion was noted (**Figure S13 – Supplementary Material**).

The hepatic architecture remained intact. Multifocal to diffuse hepatocellular cytoplasmic vacuolization, consistent with lipid accumulation and compatible with hepatic steatosis, was observed. Additional findings included mild periportal inflammatory infiltrates, focal sinusoidal edema, bile duct hyperplasia within portal tracts, and generalized hepatic congestion. No necrosis or fibrosis was observed (**Figure S14 – Supplementary Material**).

In the spleen, overall morphology was preserved. Areas of follicular lympholysis, indicating white pulp depletion, alternated with regions of lymphoid hyperplasia. Mild, generalized vascular congestion was also present (**Figure S15 – Supplementary Material**).

Collectively, these findings indicate that the observed lesions were mild and nonspecific, without evidence of marked systemic toxicity associated with CM administration.

4. Discussion

The present study aimed to evaluate the ocular tolerance of UC-MSCs CM following SbC or ITV administration in healthy male Wistar Hannover rats. By combining clinical ophthalmic examination, IOP monitoring, ERG, retinal histology, and systemic organ histological evaluation, this work provides a comprehensive assessment of local and systemic safety associated with CM delivery.

Clinical ophthalmic examinations revealed no relevant abnormalities throughout the study period, except for two cases of total mature cataracts in ITV-treated eyes. Slit-lamp and fundus evaluations remained unremarkable, and IOP values stayed within the physiological range expected for sedated Wistar rats. These findings indicate that CM administration did not induce clinically detectable ocular inflammation, structural alterations, or sustained changes in IOP, in most animals. Nevertheless, the occurrence of cataracts in the ITV group may be associated with the invasive nature of the intravitreal procedure itself, as lens injury and iatrogenic cataract formation are recognized complications of intravitreal injections. Accordingly, the SbC administration seems safer than ITV route, which has already been reported by our team (23). The low evidence of adverse clinical ocular signs further supports the overall tolerability of CM administration under the present experimental conditions.

ERG recordings after CM administration, aimed to assess potential functional alterations in retinal responses. Overall, ERG measurements revealed preservation of retinal function, as most comparisons between pre- and post-treatment regressions were not statistically significant. However, route-dependent variations were observed. ITV administration showed more frequent alterations in regression slopes, particularly in SLR and selected photopic stages, suggesting subtle modifications in retinal responsiveness. These were typically characterized by flatter post-treatment slopes or reduced amplitude increases, indicating mild alterations in photoreceptor or bipolar cell activity. In contrast, the SbC route preserved stable regression profiles before and after treatment. Temporal comparisons further suggested that early ITV-related changes tended to normalize over time, while other alterations became more apparent at later timepoints under scotopic conditions. Such patterns may reflect transient retinal adaptation, mechanical stress associated with the ITV CM administration procedure, or mild inflammatory responses

rather than a direct toxic effect of the CM itself. The volumes for each administration route were based on commonly reported ranges in rat ocular studies and were chosen to ensure procedural safety and tolerability while allowing adequate tissue exposure (24,25).

Histological assessment of the retinal tissues was consistent with the functional outcomes. Qualitative evaluation of H&E-stained sections demonstrated preserved retinal architecture across all experimental groups, with no evidence of tissue disorganization, inflammatory infiltrates, or cellular degeneration. Likewise, no relevant morphological differences were identified between OD and OS eyes. Quantitative measurements of retinal thickness further supported these findings: total retinal thickness and INL thickness remained largely unchanged following CM administration, particularly in the SbC groups. This reinforces the suitability of the OS eye as a reliable internal control in this experimental model.

In contrast, a reduction in ONL thickness was detected in the ITV groups, particularly at the later timepoint. Given that the ONL comprises the cell bodies of photoreceptors, this thinning may reflect a greater vulnerability of the outer retina to the ITV administration procedure. Notably, these alterations were not observed in animals receiving SbC administration of CM, in which retinal thickness remained stable throughout the study period. When interpreted alongside the ERG data, these findings suggest that SbC delivery induces less disruption to retinal physiology and structure than the ITV route under the conditions tested.

Systemic safety was evaluated through histopathological examination of sentinel organs (liver, kidney, and spleen). Overall, the architecture of all examined tissues was well preserved. The mild alterations identified, such as primarily vascular congestion, focal inflammatory infiltrates, and occasional degenerative changes, are frequently reported in laboratory rodents of comparable strain and age and are generally regarded as

incidental findings commonly reported in laboratory rodents of comparable strain and age (26). Importantly, no necrosis, fibrosis, or marked inflammatory lesions were observed, supporting the absence of clinically relevant systemic toxicity associated with CM administration.

Despite these encouraging findings, some limitations should be considered. The study was intentionally conducted in healthy animals to assess the ocular tolerability of hUC-MSC CM under physiological conditions. However, responses may differ in diseased retinas, where underlying pathological processes could influence the tissue response to treatment. In addition, the follow-up period was limited to 28 days. The selected timepoints (5 and 28 days) were designed to capture both early and later responses following CM administration, nevertheless, additional timepoints as well as longer observation periods would be valuable to further confirm long-term safety.

Another limitation is the absence of a sham-injected group, which could have helped to further differentiate procedure-related effects from those associated with CM. Nevertheless, the use of the contralateral eye as an internal control was considered appropriate given the invasive nature of ITV administration and the ethical principles guiding animal experimentation.

Overall, the results of the present study support the ocular and systemic tolerability of hUC-MSCs-derived CM following local ocular administration. These findings provide an important safety foundation for future studies investigating the therapeutic potential of stem cell-derived secretome in retinal diseases.

5. Conclusion

The aim of this study was to evaluate the tolerability of hUC-MSC-derived CM following SbC and ITV administration in healthy rat retinas, as a prerequisite for its safe

translation to glaucoma animal models. Taken into consideration the combined clinical, functional, structural, and systemic evaluations performed using the healthy rat model, this study supports the overall safety of ocular hUC-MSCs derived CM administration. While both delivery routes were generally well tolerated, the SbC route showed a more stable functional and structural profile. These findings suggest that SbC administration may represent a safer, easier and less disruptive strategy for CM delivery and provide a relevant experimental basis for its selection in future studies investigating the therapeutic potential of stem cell-derived secretome in experimental models of ocular diseases, such as glaucoma.

Declarations

Author Contributions: Conceptualization, A.d.S.M., E.D., R.A. and A.C.M.; methodology, A.d.S.M., B.S., G.S., R.M., I.A., J.R.M., R.A., E.D. and A.C.M.; validation, A.d.S.M., E.D., I.A., J.R.M. and A.C.M.; formal analysis, A.d.S.M., I.A., J.R.M., investigation, A.d.S.M., B.S., G.S., R.M., E.D., I.A., J.R.M., R.A., E.D. and A.C.M.; resources, A.d.S.M., I.A., J.R.M., R.A., E.D. and A.C.M.; data curation, A.d.S.M., I.A., J.R.M., R.A., E.D. and A.C.M.; writing – original draft preparation, A.d.S.M., I.A., J.R.M., R.A., E.D. and A.C.M.; writing – review and editing, A.d.S.M., B.L., A.C.S., P.S., B.S., G.S., R.M., I.A., J.R.M., R.A., E.D. and A.C.M.; visualization, A.d.S.M., B.L., A.C.S., P.S., B.S., G.S., R.M., I.A., J.R.M., R.A., E.D. and A.C.M.; supervision, E.D., R.A. and A.C.M.; project administration, E.D., R.A. and A.C.M.; funding acquisition, E.D. and A.C.M.

Funding: Alícia de Sousa Moreira (2023.00544.BD), Bruna Lopes (2021.05265.BD) and Patrícia Sousa (2023.00246.BD) acknowledge financial support from the Fundação para a Ciência e Tecnologia (FCT), Portugal. This work received financial support from the PT national funds (FCT/MECI, Fundação para a Ciência e Tecnologia and Ministério da Educação, Ciência e Inovação) through the project UID/50006/2025 DOI 10.54499/UID/50006/2025 -Laboratório Associado para a Química Verde - Tecnologias e Processos Limpos and COMPETE2030-FEDER-00716600 - NEUROBIOTECH -

Combining New Cell-based Therapies and Biodegradable Polymers to Promote Peripheral Nerve Regeneration, and from the national.

Ethics approval and consent to participate: The experimental protocol was reviewed and approved by the Animal Welfare Body (ORBEA – Organismo Responsável pelo Bem-Estar dos Animais) of the Faculty of Veterinary Medicine, University of Lisbon (ORBEA-FMV ULisboa), under protocol no. 005/2023 (approved on 14 November 2023), within the project entitled "The role of cell-based therapies in the treatment of retinal pathologies". All animal procedures complied with national legislation (Decree-Law no. 113/2013) and European regulations governing the use of animals for scientific purposes (Directive 2010/63/EU).

Human umbilical cord-derived mesenchymal stromal cells (hUC-MSCs) were obtained from a certified commercial supplier (PromoCell®, Heidelberg, Germany). According to the manufacturer's documentation, all biological materials were collected from donors who had provided informed consent, and tissue procurement was conducted in accordance with applicable ethical and legal requirements. Clinical trial number: not applicable.

Consent for publication: All participants provided informed consent for publication.

Data Availability: The data that support the results of this study are available on this article; other information are available under reasonable request. No study protocol was prospectively registered.

Code Availability: No custom code was generated for this study.

Materials Availability: Not applicable.

Acknowledgments: The authors would like to acknowledge Inês Dias for her invaluable assistance with animal care, including maintenance of housing conditions, feeding and support. Her contribution was essential to ensure the proper management and welfare of the animals throughout the study.

The authors also thank Beatriz Azevedo (Laboratory of Pathological Anatomy, Faculty of Veterinary Medicine, University of Lisbon) for her assistance in histological sample preparation. The authors used an AI-based language model (ChatGPT, OpenAI) to assist with language editing and improvement of manuscript clarity. All scientific content, data analysis, interpretation, and conclusions were developed by the authors.

Conflicts of Interest: The authors declare no conflicts of interest.

Abbreviations

The following abbreviations are used in this manuscript:

CM: Conditioned Medium
DMEM(/F12): Dulbecco's Modified Eagle Medium (/Ham's F12)
ERG: Electroretinography
GCL: Ganglion Cell Layer
(h)UC-MSC(s): (Human) Umbilical Cord Mesenchymal Stromal Cell(s)
H&E: Hematoxylin and Eosin
Hz: Hertz
INL: Inner Nuclear Layer
IOP: Intraocular Pressure
ITV: Intravitreal
MSC(s): Mesenchymal Stromal Cell(s)
OD: Oculus Dexter (right eye)
ONL: Outer Nuclear Layer
OS: Oculus Sinister (left eye)
PA: Photopic Adaptation
PBS: Phosphate Buffered Saline
PF: Photopic Flicker
PLR: Photopic Luminescent Response
R^2: Coefficient of Determination
RGC(s): Retinal Ganglion Cell(s)
SA: Scotopic Adaptation
SbC: Subconjunctival
SD: Standard Deviation
SEM: Standard Error of the Mean
SLR: Scotopic Luminescent Response
µL: Microliter
µV: Microvolt

References

1. Quigley HA. Glaucoma: Macrocosm to microcosm. The Friedenwald Lecture. Invest Ophthalmol Vis Sci. 2005;46(8):2663–70. doi:10.1167/iovs.04-1070 PubMed PMID: 16043835.

2. Tham YC, Li X, Wong TY, Quigley HA, Aung T, Cheng CY. Global prevalence of glaucoma and projections of glaucoma burden through 2040: A systematic review and meta-analysis. Ophthalmology. 2014;121(11):2081–90. doi:10.1016/j.ophtha.2014.05.013 PubMed PMID: 24974815.

3. Quigley H, Broman AT. The number of people with glaucoma worldwide in 2010 and 2020. British Journal of Ophthalmology. 2006;90(3):262–7. doi:10.1136/bjo.2005.081224 PubMed PMID: 16488940.

4. Gelatt KN, MacKay EO. Secondary glaucomas in the dog in North America. Vet Ophthalmol. 2004;7(4):245–59. doi:10.1111/j.1463-5224.2004.04034.x PubMed PMID: 15200621.

5. Gelatt KN, MacKay EO. Prevalence of the breed-related glaucomas in pure-bred dogs in North America. Vet Ophthalmol. 2004;7(2):97–111. doi:10.1111/j.1463-5224.2004.04006.x PubMed PMID: 14982589.

6. Chang EE, Goldberg JL. Glaucoma 2.0: Neuroprotection, Neuroregeneration, Neuroenhancement. Ophthalmology. 2012 May;119(5):979. doi:10.1016/J.OPHTHA.2011.11.003 PubMed PMID: 22349567.

7. de Sousa Moreira A, Lopes B, Sousa AC, Coelho A, Sousa P, Araújo A, et al. Stem Cell-Based Therapies for Glaucoma Treatment: A Review Bridging the Gap in Veterinary Patients. Int J Mol Sci. 2024 Jan 1;26(1). doi:10.3390/IJMS26010232 PubMed PMID: 39796087.

8. Almasieh M, Zhou Y, Casanova C, Polo A Di. Structural and functional neuroprotection in glaucoma: role of galantamine-mediated activation of muscarinic acetylcholine receptors. Cell Death Dis. 2010;27. doi:10.1038/cddis.2009.23

9. Harrell CR, Fellabaum C, Arsenijevic A, Markovic BS, Djonov V, Volarevic V. Therapeutic Potential of Mesenchymal Stem Cells and Their Secretome in the Treatment of Glaucoma. Stem Cells Int. 2019;2019. doi:10.1155/2019/7869130 PubMed PMID: 31949441.

10. Sharun K, Banu SA, Alifsha B, Abualigah L, Pawde AM, Dhama K, et al. Mesenchymal stem cell therapy in veterinary ophthalmology: clinical evidence and prospects. Veterinary Research Communications 2024 48:6. 2024 Aug 30;48(6):3517–31. doi:10.1007/s11259-024-10522-w PubMed PMID: 39212813.

11. Kalinski P. Regulation of immune responses by prostaglandin E2. Journal of Immunology. 2012;188(1):21–8. doi:10.4049/jimmunol.1101029

12. Tögel F, Weiss K, Yang Y, Hu Z, Zhang P, Westenfelder C. Vasculotropic, paracrine actions of infused mesenchymal stem cells are important to the recovery from acute kidney injury. Am J Physiol Renal Physiol. 2007;292:1626–35. doi:10.1152/ajprenal.00339.2006.-Acute

13. Suga H, Eto H, Shigeura T, Inoue K, Aoi N, Kato H, et al. IFATS Collection: Fibroblast Growth Factor-2-Induced Hepatocyte Growth Factor Secretion by Adipose-Derived Stromal Cells Inhibits Postinjury Fibrogenesis Through a c-Jun N-Terminal Kinase-Dependent Mechanism. Stem Cells. 2009;27(1):238–49. doi:10.1634/stemcells.2008-0261

14. Gunawardena TNA, Rahman MT, Abdullah BJJ, Abu Kasim NH. Conditioned media derived from mesenchymal stem cell cultures: The next generation for regenerative medicine. J Tissue Eng Regen Med. 2019 Apr 1;13(4):569–86. doi:10.1002/term.2806 PubMed PMID: 30644175.

15. Bouche Djatche WH, Zhu H, Ma W, Li Y, Li Z, Zhao H, et al. Potential of mesenchymal stem cell-derived conditioned medium/secretome as a therapeutic option for ocular diseases. Regenerative Med. 2023 Oct 1;18(10):795–807. doi:10.2217/RME-2023-0089;PAGE:STRING:ARTICLE/CHAPTER PubMed PMID: 37702008.

16. Noronha NDC, Mizukami A, Caliári-Oliveira C, Cominal JG, Rocha JLM, Covas DT, et al. Priming approaches to improve the efficacy of mesenchymal stromal cell-based therapies. Stem Cell Res Ther. 2019;10(131):1–21. doi:10.1186/s13287-019-1259-0 PubMed PMID: 31101067.

17. Valencia J, Yáñez RM, Muntión S, Fernández-García M, Martín-Rufino JD, Zapata AG, et al. Improving the therapeutic profile of MSCs: Cytokine priming reduces donor-dependent heterogeneity and enhances their immunomodulatory capacity. Front Immunol. 2025 Feb 17;16:1473788. doi:10.3389/FIMMU.2025.1473788/BIBTEX PubMed PMID: 40034706.

18. Pereira T, Ivanova G, Caseiro AR, Barbosa P, Bártolo PJ, Santos JD, et al. MSCs conditioned media and umbilical cord blood plasma metabolomics and composition. PLoS One. 2014 Nov 25;9(11). doi:10.1371/JOURNAL.PONE.0113769 PubMed PMID: 25423186.

19. Caseiro AR, Pedrosa SS, Ivanova G, Branquinho MV, Almeida A, Faria F, et al. Mesenchymal Stem/ Stromal Cells metabolomic and bioactive factors profiles: A comparative analysis on the umbilical cord and dental pulp derived Stem/ Stromal Cells secretome. PLoS One. 2019 Nov 1;14(11). doi:10.1371/JOURNAL.PONE.0221378, PubMed PMID: 31774816.

20. Caseiro AR, Pereira T, Ivanova G, Luís AL, Maurício AC. Neuromuscular Regeneration: Perspective on the Application of Mesenchymal Stem Cells and Their Secretion Products. Stem Cells Int. 2016;2016:1–16. doi:10.1155/2016/9756973

21. Attar M, Brassard JA, Kim AS, Matsumoto S, Ramos M, Vangyi C. Safety Evaluation of Ocular Drugs. A Comprehensive Guide to Toxicology in Preclinical Drug Development. 2013;567–617. doi:10.1016/B978-0-12-387815-1.00024-1

22. Silva B, Gonçalves LM, Braz BS, Delgado E. Chitosan and Hyaluronic Acid Nanoparticles as Vehicles of Epoetin Beta for Subconjunctival Ocular Delivery. Mar Drugs. 2022 Feb 1;20(2). doi:10.3390/md20020151 PubMed PMID: 35200680.

23. Resende AP, São-Braz B, Delgado E. Alternative route for erythropoietin ocular administration. Graefes Arch Clin Exp Ophthalmol. 2013 Aug;251(8):2051–6. doi:10.1007/s00417-013-2367-7 PubMed PMID: 23702929.

24. Martínez-Vacas A, Di Pierdomenico J, Gómez-Ramirez AM, Vidal-Sanz M, Villegas-Pérez MP, García-Ayuso D. Dose-Related Side Effects of Intravitreal Injections of Humanized Anti-Vascular Endothelial Growth Factor in Rats: Glial Cell Reactivity and Retinal Ganglion Cell Loss. Invest Ophthalmol Vis Sci. 2024 Apr 1;65(4):10. doi:10.1167/IOVS.65.4.10 PubMed PMID: 38573620.

25. Mo L, Deng M, Chen J, Huai S, Du L, Xu X, et al. Subconjunctival injection of rapamycin-loaded polymeric microparticles for effective suppression of noninfectious uveitis in rats. Int J Pharm. 2024 May 25;657:124178. doi:10.1016/J.IJPHARM.2024.124178 PubMed PMID: 38692499.

26. Cooper TK, Meyerholz DK, Beck AP, Delaney MA, Piersigilli A, Southard TL, et al. Research-Relevant Conditions and Pathology of Laboratory Mice, Rats, Gerbils, Guinea Pigs, Hamsters, Naked Mole Rats, and Rabbits. ILAR J. 2022;62(1–2):77. doi:10.1093/ilar/ilab022 PubMed PMID: 34979559.

Tables

Table 1. P-values of slope comparisons (Before vs. After) obtained from linear regression analyses of ERG a- and b-waves across all steps and experimental groups. Significant differences ($p < 0.05$) are shown in bold and marked with an asterisk (*).

ERG step	Wave	SbC 5 days *p* (slopes)	ITV 5 days *p* (slopes)	SbC 28 days *p* (slopes)	ITV 28 days *p* (slopes)
SLR	b	0.5120	0.1466	0.3462	**0.0074***
SLR	a	0.1554	**<0.0001***	0.0753	**<0.0001***
PA	b	0.5560	0.6570	0.7396	0.1820
PA	a	0.4952	0.2099	0.1940	0.0785
PLR	b	0.8429	**0.0265***	0.3711	0.0993
PLR	a	0.7269	0.7449	0.9556	0.2333
PF	b	0.3400	**0.0251***	0.9367	0.9292
PF	a	0.7697	0.5447	0.5322	0.2899
SA	b	0.4120	0.4536	0.7931	0.5475
SA	a	0.7337	0.6783	**0.0129***	0.6890

Supplementary Files

This is a list of supplementary files associated with this preprint. Click to download.

- SupplementaryMaterialfigures.docx